A New Receiver Architecture for MIMO Beam-Forming Applications

Yucheng Dai*, Yahia R. Ramadan*, Hlaing Minn*, Jiu Xiong*, Jin Liu* and Alan Gatherer†
* Department of Electrical and Computer Engineering, University of Taxes at Dallas, Richardson, TX.
†Huawei Technologies Co., Plano, TX.
Email: {yxd140430, yrr160030, hxm025000, jxx130530, jinliu}@utdallas.edu, Alan.Gatherer@huawei.com

***Abstract*—Owing to its reduction in hardware complexity and power consumption, hybrid beam-forming has become one of the most promising substitutes for fully digital beam-forming (FDB) in large antenna array systems. In conventional hybrid beam-forming (CHB) architecture, phase shifters are designed to operate at RF band and inaccuracies of the RF phase shifts are unavoidable in practice. Furthermore, these RF phase shifters still consume considerable power if implemented as active devices or a large space/area on dice (form factor) if implemented as passive devices. This issue becomes more critical for massive MIMO systems where lower power consumption and smaller form factor are much desired due to the large number of antenna elements. Aiming at reducing power consumption and form factor of the receiver, we investigate a new method to insert phase shifts via adjusting sampling-offset on sample and hold (S&H) circuit. Based on this method, a new receiver architecture with RF under-sampling technique and adjustable S&H circuit is proposed. We also develop a method to find out the required phase shifts for the beam-forming in the proposed receiver architecture. Performance evaluation at 28 GHz band shows that the proposed technology gives practically the same bit error rate (BER) performance as the CHB architecture but yields advantages in terms of power consumption, chip area, and beam-forming phase errors, which makes it appealing for massive MIMO systems.**

I. Introduction

In response to increasing demand of high data rate communication, more spectrum resources at higher frequency (e.g., 28 GHz) are recently allocated to cellular systems. However, the higher frequency band causes larger propagation losses. Benefited from the increase in RF frequency and corresponding decrease in antenna size, accommodating more antennas per device/equipment is practical [1]. Applying beam-forming with more antennas can compensate for the propagation losses. Recently, systems with 32×32 or even more antennas [2] are considered in 28 GHz band to meet different requirements in BER, QoS and latency.

In large antenna array systems, beam-forming architecture is one of the most critical issues that affect system performance such as BER and power consumption. FDB architecture is considered to be the best candidate for BER performance as it can achieve highest beam-forming gain for a given number of antennas. Nevertheless, due to hardware and cost issues, application of the FDB architecture with acceptable power consumption and layout size is not likely to be practical for large antenna array systems [1]. An alternative architecture, namely hybrid beam-forming architecture, is proposed in [3]. This architecture reduces the needed number of RF chains via combining the signals from different antennas before passing the RF chain. However, hybrid beam-forming architecture inevitably requires RF phase shifters, which would suffer either high power consumption or large form factor. Therefore, a more efficient architecture is needed to accomplish phase shifts in RF beam-forming.

This work was supported in part by a gift from Huawei, Plano, TX, USA.

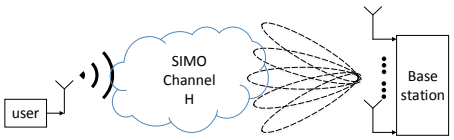

Fig. 1. The considered system model consisting of a base station with a large antenna array

One way to introduce a phase shift to the received baseband signal is to exploit the phase of RF or IF carrier signal. If the carrier frequency is much larger than the signal bandwidth, the baseband signal is constant during one period of the carrier T_c. Then, if we intentionally introduce a time offset while sampling the received signal and removing the carrier signal as usual, an extra phase will be left in the demodulated baseband signal. A similar idea can be found in [4] where the authors shift the phase (or delay) of the signal from the local oscillator to achieve required phase shifts in the baseband. However, more mixers are needed for inserting phase shifts via IF sampling compared to the CHB architecture if normal super-heterodyne receiver architectures are considered. On the other hand, direct RF sampling at the Nyquist or higher rate of the RF signal is not practical due to limited speed of analog digital converter (ADC). Therefore, aiming to avoid using unnecessary mixers and impractical ADC, we apply RF under-sampling technique based on [5], which is also known as band-pass sampling or sampling mixer. By choosing a proper sampling frequency f_s, this technique can down-convert the pass-band signal to a desired IF band, without requiring a mixer. To avoid aliasing from other bands, it uses a high performance bandpass filter before S&H module.

Scope and Contributions: In this paper, we consider an uplink OFDM system with a large antenna array at the base station. The system model is shown in Fig. 1 where the user has only one omni-directional antenna while the base station has an antenna array to implement beam-forming. The

main technical contribution of this paper is a new receiver architecture of base station with novel adjustable S&H circuit that can replace low-performance phase shifters in the RF band. The proposed architecture applies an RF under-sampling technique combined with appropriately designed sampling offsets, as a way of accomplishing the tasks of joint phase shift insertion and down-conversion mixers. In addition, the channel estimation and corresponding beam-forming phase generation of this new architecture is presented in details. Our performance evaluation results demonstrate the advantages of the proposed technology in terms of power consumption, chip area (form-factor) and beam-forming phase errors.

The rest of the paper is organized as follows. Section II briefly describes the existing receiver architectures. Section III explains the concept of phase shift insertion through RF sampling offset. Then, Section IV details the proposed sampling-shift based beam-forming architecture as well as related channel estimation and beam-forming phase generation algorithm. Section V presents performance evaluation results and Section VI provides conclusions.

II. Existing System Architectures

Among all the existing beam-forming system architectures, three widely considered architectures can be chosen as representatives, namely FDB architecture, CHB fully connected architecture and CHB sub-array architecture. For an antenna array system with N_{ant} antennas, we need the number of RF chains $N_{\text{RF}} = N_{\text{ant}}$ to apply the FDB architecture, which incurs high power consumption and equipment cost. On the other hand, if the CHB fully connected architecture is applied, we can choose any N_{RF} as long as the condition $1 < N_{\text{RF}} \leq N_{\text{ant}}$ is met. The CHB sub-array architecture, which shares the same constraint of N_{RF} as the fully connected architecture, has its unique constraint as $\sum_{j=1}^{N_{\text{RF}}} \beta_j = N_{\text{ant}}$, where β_j denotes the number of antennas in the jth sub-array. To simplify the beam-forming calculation, we often choose β_j to be the same among all sub-arrays. The above description indicates that both of the two CHB architectures require less RF chains than the FDB architecture does and the main difference between them is the analog beam-forming module.

A typical architecture of analog beam-forming module can be described as follows. The signals from antennas are reshaped by phase shifters and variable gain amplifier (VGA), then the outputs are summed up and forwarded to RF chains. In the fully connected architecture, the number of phase shifters or VGA in the analog beam-forming module is $N_{\text{RF}} \cdot N_{\text{ant}}$ while in the sub-array architecture, this number becomes N_{ant}, which is much less than the previous one if a large N_{RF} is chosen. Thus, to save power and simplify beam-former design, we consider the CHB with sub-array architecture as our referenced design in this paper. In addition, [6] proposes an architecture that can realize the function of VGA by two phase shifters and an adder. Meanwhile, [7] points out that performance gain of analog beam-forming modules with both VGA and phase shifters over the ones with phase shifters only is small. Thus, for the purpose of our investigation, we just consider using phase shifters only analog beam-forming module.

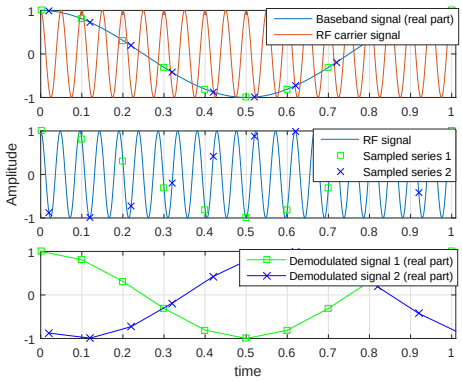

Fig. 2. Phase insertion via sampling offset

III. Phase Shift Generation via Sampling Offset

In this section, we illustrate the basic idea of inserting phase shift through sampling offset. For a complex baseband signal $s_{\text{BB}}(t)$, the corresponding quadrature-modulated passband signal can be represented as:

$$s_{\text{PB}}(t) = \Re[s_{\text{BB}}(t)e^{j2\pi f_c t}] \tag{1}$$

where f_c is the carrier frequency and $\Re[*]$ denotes the real part. Let us consider RF sampling of $s_{\text{PB}}(t)$ using the following two impulse streams $p_1(t)$ and $p_2(t)$ with a time offset ΔT between them:

$$\begin{aligned} p_1(t) &= \sum_{n=-\infty}^{+\infty} \delta(t - nT_{\text{s}}) \\ p_2(t) &= \sum_{n=-\infty}^{+\infty} \delta(t - nT_{\text{s}} - \Delta T) \end{aligned} \tag{2}$$

where T_{s} is the RF sampling interval. Thus, the sampled signal of $s_{\text{PB}}(t)$ with the pulse stream $p_1(t)$ is given by

$$\begin{aligned} \hat{s}_{\text{PB},1}(t) &= s_{\text{PB}}(t)p_1(t) \\ &= \sum_{n=-\infty}^{+\infty} \Re[s_{\text{BB}}(nT_{\text{s}})e^{j2\pi f_c nT_{\text{s}}}]\delta(t - nT_{\text{s}}). \end{aligned} \tag{3}$$

Similarly, we can have the sampled signal with the pulse stream $p_2(t)$ as

$$\begin{aligned} \hat{s}_{\text{PB},2}(t) = \sum_{n=-\infty}^{+\infty} &\Re[s_{\text{BB}}(nT_s + \Delta T)e^{j2\pi f_c \Delta T} \cdot e^{j2\pi f_c nT_s}] \\ &\cdot \delta(t - nT_s - \Delta T). \end{aligned} \tag{4}$$

After a proper carrier frequency removing procedure, the demodulated baseband signals are

$$\hat{s}_{\text{BB},1}(nT_{\text{s}}) = s_{\text{BB}}(nT_{\text{s}}) \tag{5}$$

$$\hat{s}_{\text{BB},2}(nT_{\text{s}} + \Delta T) = s_{\text{BB}}(nT_{\text{s}} + \Delta T)e^{j2\pi f_c \Delta T}. \tag{6}$$

If ΔT is small enough (i.e., $\Delta T \ll \frac{1}{\text{B}_{\text{W}}}$, where B_{W} is the bandwidth of the baseband signal), we have $s_{\text{BB}}(nT_{\text{s}}) \approx s_{\text{BB}}(nT_{\text{s}} + \Delta T)$ and hence

$$\hat{s}_{\text{BB},2}(nT_{\text{s}} + \Delta T) \approx s_{\text{BB}}(nT_{\text{s}})\ e^{j2\pi f_c \Delta T}. \tag{7}$$

Then, one can observe from (7) that a $2\pi f_c \Delta T$ phase shift is inserted in the baseband signal via a sampling offset ΔT.

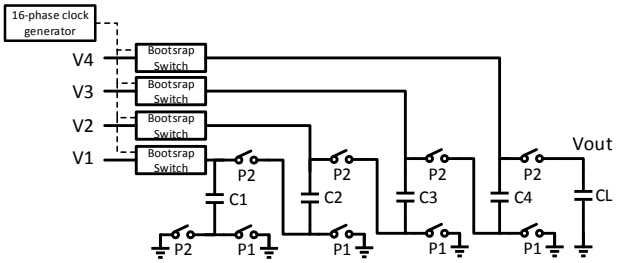

Fig. 3. Proposed S&H circuit with offset time generation module

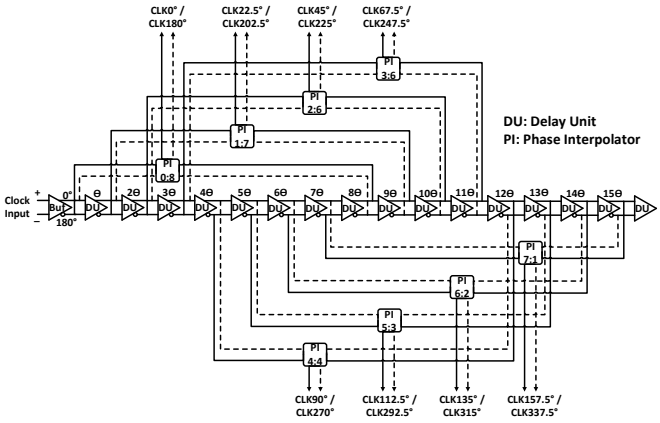

Fig. 4. Proposed multi-phase clock generator

Fig. 2 shows a simple example of phase shift insertion via a sampling offset. To cover any possible phase shift, we usually pick $\Delta T_{\max} = T_c$, so that $0 \leq 2\pi f_c \Delta T \leq 2\pi$ can be achieved. Fig. 3 shows the hardware design for the proposed S&H circuit with a time offset generation and control module. The main procedure of this part is listed below:

1) According to the phase resolution requirement, a series of clock signals with certain time offsets are generated from the multi-phase clock generator.

2) Based on the phase shift we need to insert, the corresponding clock signal is used to trigger the sampling. During this period, P1 switches are closing while P2 switches are opening so that the signals from antennas are sampled with their own offsets respectively.

3) After sampling, P1 switches will open and P2 switches will close to combine the sampled analog signals within each sub-array and pass them through quantization module.

Fig. 4 shows the circuit for multi-phase clock generator. The original clock signal is passed through several delay units and then combined by phase interpolators to generate clock signals with required offsets.

IV. Proposed Beam-forming System

A. System configuration

Consider a base station with $N_{\rm r}$ antennas and a single-antenna user[I] using OFDM with N_c sub-carriers. When the user transmits symbol x_i on sub-carrier i, the corresponding

[I]Due to space limitation, we omitted the proposed architecture design for multiuser case as future work.

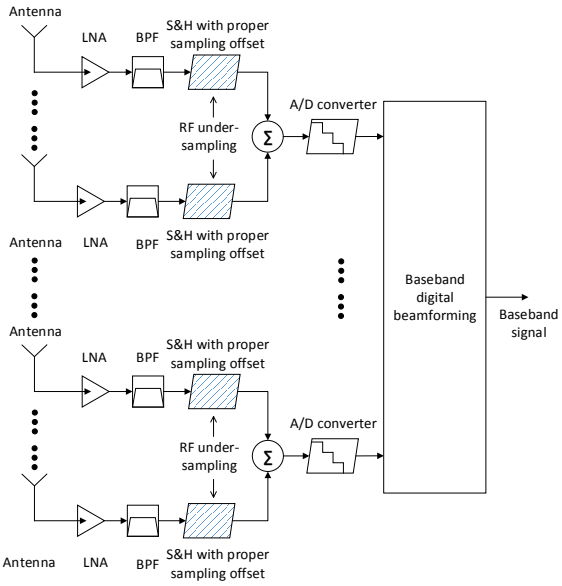

Fig. 5. Proposed base station receiver architecture

$N_{\rm r} \times 1$ received vector $\mathbf{y}_i$ (collected from all antennas) can be given as

$$\mathbf{y}_i = \mathbf{H}_i x_i + \mathbf{n}_i \tag{8}$$

where $\mathbf{n}_i$ and $\mathbf{H}_i$ represent the $N_{\rm r} \times 1$ noise vector and complex channel gain vector on sub-carrier i, respectively. With an appropriate OFDM parameter setting, each sub-carrier experiences a frequency flat channel. Then, if the FDB architecture is applied, the received symbol z_i after receive beam-forming is

$$z_i = \mathbf{w}_{\text{fully},i}\mathbf{y}_i = \mathbf{w}_{\text{fully},i}(\mathbf{H}_i x_i + \mathbf{n}_i) \tag{9}$$

where $\mathbf{w}_{\text{fully},i}$ denotes the $1 \times N_{\rm r}$ FDB beam-former vector. On the other hand, if the hybrid beam-forming sub-array architecture with $N_{\rm RF}$ RF chains is applied, the prior equation can be reformulated as

$$z_i = \mathbf{w}_{\text{BB},i}\mathbf{W}_{\rm RF}(\mathbf{H}_i x_i + \mathbf{n}_i) \tag{10}$$

where $\mathbf{w}_{\text{BB},i}$ is a $1 \times N_{\rm RF}$ baseband beam-forming vector and $\mathbf{W}_{\rm RF}$ is a $N_{\rm RF} \times N_{\rm r}$ RF beam-forming matrix. As we consider sub-array and phase shifter only architecture at the base station side, the non-zero elements of $\mathbf{W}_{\rm RF}$ lie in corresponding positions where connections between antennas and RF chains exist and they have unit gain with specific phases according to the beam-forming design. The proposed approach implements (10) by a new sampling-shift RF sub-sampling approach and the corresponding base station receiver architecture is shown in Fig. 5. Note that sampling is an integral part of ADC in the existing approaches while our approach splits the sampling part (S&H) out of our ADC.

B. Channel estimation

Compared to FDB architecture receivers, hybrid beam-forming architecture receivers face more challenges in estimating all individual channels as the number of RF chains is less than the number of antennas, which means not all individual signals of different antennas are separately reachable

simultaneously. Furthermore, this procedure requires not only considerable accuracy but also low calculation complexity and latency to generate the RF beam-former within the coherent time of the channel. To achieve a balance between the latency and accuracy of the estimation, we need to exploit the characteristics of mm-Wave band channel. Unlike UHF and lower frequency bands, the signals in the mm-Wave band bear severe path loss and reflection loss. Thus, it is commonly assumed that channel impulse response (CIR) of mm-Wave channel would be sparse in time domain and spatial domain [8]. Another critical observation about mm-Wave channels, as a result of the decrease in distance between antennas, is that the antennas in the same array share identical path gain while the array responses are different, which are determined by AoA of the signals and positions of the antennas. Based on such characteristics, we propose a frequency domain least square channel estimation method. From Eq. (8), we can represent the relationship between transmitted symbol x_i and received symbol $y_{l,i}$ on antenna l and sub-carrier i as

$$y_{l,i} = x_i H_{l,i} + n_{l,i} \tag{11}$$

where $H_{l,i}$ and $n_{l,i}$ are complex channel gain and noise on sub-carrier i and antenna l, respectively. Thus, the least square estimation of $H_{l,i}$ based on observed $y_{l,i}$ is

$$\hat{H}_{l,i} = \frac{y_{l,i} x_i^*}{|x_i|^2}. \tag{12}$$

On the other hand, the frequency domain channel $H_{l,i}$ can be derived from the time domain channel as

$$H_{l,i} = \sum_{p=1}^{K} \alpha_p \varphi_{p,l} \exp[\frac{-j2\pi(i-1)\tau_p}{N_c}] \tag{13}$$

where α_p, τ_p, $\varphi_{p,l}$ are the complex gain, relative delay and array response of path p and antenna l, respectively, and K is the total number of paths. This equation indicates a fact that for the same path, the signals on different antennas vary only in phases which are derived from the phase differences between array responses of this path. As we know, for path p with azimuth AoA ϕ_p and zenith AoA θ_p, the array response $\varphi_{p,l}$ can be expressed as

$$\varphi_{p,l} = \exp\{-\frac{2\pi j}{\lambda} \begin{bmatrix} \sin(\theta_p)\cos(\phi_p) \\ \sin(\theta_p)\sin(\phi_p) \\ \cos(\theta_p) \end{bmatrix}^{\mathrm{T}} \mathbf{p}_l\} \tag{14}$$

where $\mathbf{p}_l$ denotes the antenna location vector and λ denotes the wave-length of the carrier. Then, we can see that for antenna j, k and l, if their location vectors satisfy

$$\mathbf{p}_j - \mathbf{p}_k = \mathbf{p}_k - \mathbf{p}_l, \tag{15}$$

then the corresponding array response of path p between different antennas will have the relationship:

$$\frac{\varphi_{p,j}}{\varphi_{p,k}} = \frac{\varphi_{p,k}}{\varphi_{p,l}}. \tag{16}$$

It can be concluded from (13) that if the channel is sparse in time and spatial domain (e.g., dominant paths share similar AoA), the phase difference of $H_{l,i}$ and $H_{k,i}$ of antenna l and k is the same for all sub-carrier i and is mainly determined by their phase difference of array responses to the dominant paths. Under this circumstance, we can expect the same RF beam-former can achieve the same beam-forming gain among all sub-arrays as long as the relative positions of the antennas within the sub-array are identical. Thus, we can formulate a simple and low-overhead channel estimation and RF beam-former design strategy which exploits the aforementioned relation.

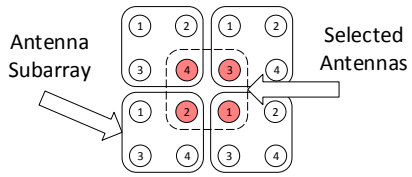

Fig. 6. Antenna selection plan which holds the same relative antenna positions as the antennas in each sub-array

The proposed strategy is illustrated by an example with 16 antennas which are structured into four sub-arrays of size 2×2 each, as shown in Fig. 6. With one ADC for each sub-array, simultaneous estimation of the individual channels of the antennas within the sub-array is infeasible. Thus, for channel estimation, we select the four antennas in red which are connected to four different ADCs. Since the relative positions of the antennas in red are the same as those of the antennas within each sub-array, the RF beam-former for one group of antennas is suitable for another group of antennas too. During the channel estimation phase, only the S&H outputs of those antennas in red are forwarded to their respective ADCs and those of the other antennas are grounded (effectively disconnected to their ADCs). By this, we remove the contamination from other antennas to the channel estimation of the red antennas. We first obtain channel estimates of the antennas in red based on pilot signals, construct RF beam-former based on the obtained channel knowledge and then apply this beam-former to all four sub-arrays.

C. Beam-forming phase generation algorithm

In this section, we introduce a beam-forming phase generation method based on the channel estimates. Our goal here is to build the RF beam-former $\mathbf{W}_{\mathrm{RF},I_m}$ to maximize the average SNR across sub-carriers as

$$\mathbf{W}_{\mathrm{RF},I_m} = \underset{\mathbf{W}_{\mathrm{RF},I_m}}{\arg\max} \frac{1}{N_c} \sum_{i=1}^{N_c} \gamma_{i,I_m} \tag{17}$$

where I_m means the vector of the antenna indexes belonging to sub-array m and γ_{i,I_m} is the receiver side SNR after RF beam-forming of sub-carrier i and sub-array m given as

$$\gamma_{i,I_m} = \|\mathbf{W}_{\mathrm{RF},I_m}^{\mathrm{H}} \mathbf{H}_{I_m,i}\|^2 \frac{\mathrm{P_T}}{\sigma_{\mathrm{N}}^2} \tag{18}$$

where $\mathrm{P_T}$ and σ_{N}^2 are the transmitted power and noise power of each sub-carrier. The problem can be simplified as

$$\mathbf{W}_{\mathrm{RF},I_m} = \underset{\mathbf{W}_{\mathrm{RF},I_m}}{\arg\max} \sum_{i=1}^{N_c} \|\mathbf{W}_{\mathrm{RF},I_m}^{\mathrm{H}} \mathbf{H}_{I_m,i}\|^2. \tag{19}$$

The solution can be derived as

$$\mathbf{W}_{\mathrm{RF},I_m}^{\mathrm{H}} = \mathrm{eigs}(\sum_{i=1}^{N_c} \mathbf{H}_{I_m,i} \mathbf{H}_{I_m,i}^{\mathrm{H}}, 1) \tag{20}$$

where $\mathrm{eigs}(\mathbf{A}, N)$ means taking the eigenvectors of $\mathbf{A}$ with first N largest eigenvalues. In addition, as no VGA is applied in system, we can use an approximate of the optimal beam-forming vector $\widetilde{\mathbf{W}}^{\mathrm{H}}_{\mathrm{RF},I_m}$ and the corresponding phase offset vector $\boldsymbol{\theta}_{\mathrm{RF},I_m}$ as

$$\begin{array}{rcl} \widetilde{\mathbf{W}}^{\mathrm{H}}_{\mathrm{RF},I_m} & \approx & \exp\left(j\angle \mathbf{W}^{\mathrm{H}}_{\mathrm{RF},I_m}\right) \\ \boldsymbol{\theta}_{\mathrm{RF},I_m} & \approx & \angle \mathbf{W}^{\mathrm{H}}_{RF,I_m}. \end{array} \tag{21}$$

For scenarios where the dominant channel paths center around a single AoA, we can average the phase difference vector across different sub-arrays to suppress the effects of noise and to simplify phase offset computation and generation (with much lower complexity). Then, we have

$$\boldsymbol{\theta}_{\mathrm{RF}} = \frac{1}{M}\sum_{m=1}^{M} \boldsymbol{\theta}_{\mathrm{RF},I_m} \tag{22}$$

where M denotes the total number of subarrays in the system. Since the generated phase shifts should have limited resolution for practical implementation, we need to quantize $\boldsymbol{\theta}_{\mathrm{RF}}$. For a phase resolution of r_{res} bits, the step-size in phase quantization is $\theta_{\mathrm{step}} = 2\pi/2^{r_{\mathrm{res}}}$. Then, the initial quantized vector of $\boldsymbol{\theta}_{\mathrm{RF}}$ can be derived as

$$\mathbf{d}_0 = \lfloor \boldsymbol{\theta}_{\mathrm{RF}}/\theta_{\mathrm{step}} \rfloor. \tag{23}$$

Since $\mathbf{d}_0$ is truncated, the quantized phase offset vector that is closest to $\boldsymbol{\theta}_{\mathrm{RF}}$ lies in

$$\mathbf{s} = [d_{0,1} + s_1, d_{0,2} + s_2, \ldots, d_{0,F} + s_F], s_i \in \{0, 1\} \tag{24}$$

where F is the number of antennas in sub-array m. Then, we design the quantized phase offset vector $\mathbf{s}_{\mathrm{c}}$ by maximizing the projection of the quantized beam-forming vector to the unquantized beam-forming vector as

$$\mathbf{s}_{\mathrm{c}} = \arg\max_{\mathbf{s}} |\exp[-j\ \theta_{\mathrm{step}} \cdot \mathbf{s}^T] \exp[j\ \boldsymbol{\theta}_{\mathrm{RF}}]| \tag{25}$$

where the variables in optimizing $\mathbf{s}$ are $\{s_i\}$ in (24). For a sub-array with $F = 4$ antennas, the above optimization just needs to compare $2^F = 16$ candidate points, thus having very low complexity.

V. Performance evaluation

In the section, BER results of different scenarios are provided and evaluated. In simulation, we use 28 GHz non-line-of-sight channel model proposed by NYU wireless lab [8]. For simplicity, we consider using zero-forcing beam-former in the baseband. To have the channel estimated well, we assume that the user transmits five OFDM symbols for channel estimation for RF beam-forming and another five OFDM symbols for estimating the equivalent channel after RF beam-forming. In addition, for comparison purpose, we assume that the distance between users and base station and shadowing factor are fixed, therefore the instantaneous SNR at receiver side is fixed. Other simulation parameters are shown in Table I.

Fig. 7 demonstrates the BER results of the proposed architecture with different phase resolutions. The FDB architecture which requires much higher power consumption and hardware complexity is also included as a reference. This figure indicates that the better resolution of the phase offsets leads to better BER performance. In addition, the proposed architecture gains some advantages over the FDB architecture when SNR is less than -5 dB. This phenomenon can be explained as follows. The channel estimation of individual antennas for the FDB architecture in the low SNR region is not reliable and thereby the beam-forming based on poor channel estimates leads to poor BER performance. On the other hand, in the proposed architecture, the RF beam-forming provides a boost in SNR of the equivalent channels after RF beam-forming. This SNR boost (and hence better quality of the channel estimate) appears to be greater than the SNR loss due to less RF chains, thus yielding slight BER advantage over the FDB in the low SNR region. Also note that massive MIMO systems are expected to operate at a relatively low SNR region (for energy efficiency) where the proposed architecture with even 2 or 3 bit phase offset resolution offers a more attractive solution than the FDB approach.

TABLE I
Simulation parameters

Parameters	Value
# of antennas at base station N_{r}	64
# of RF chains at base station N_{RF}	16
Sub-array size	2×2
# of antennas at user side	1
Modulation type	16-QAM
OFDM DFT size	2048
CP length	512
Sub-carrier spacing	480 kHz
RF carrier frequency f_{c}	28 GHz
baseband signal bandwidth $\mathrm{B_w}$	$\sim$500 MHz(1032 used sub-carriers)
Receiver noise figure	10 dB
ADC sampling frequency f_{s}	3.9322 GHz
IF frequency f_{IF}	474.88 MHz
ADC resolution	6 bits
Transmit power	1 watt
RMS sampling jitter	0.2 ps

Next, Fig. 8 shows the BER results of the proposed architecture along with the existing architectures in [9], [10], [11], [12], [13] and [14] which implement phase shifters in RF beam-forming. To observe the relationship between different methods clearly, the zoomed-in results are also shown. The figure shows that our proposed phase generation method can achieve practically the same BER performance as the referenced phase shifters do, if not better.

Finally, we compare power consumption, circuit area and root-mean-square phase errors of different RF phase-shift generation architectures in Table II. We observe that the proposed phase generation method uses less power than the active phase shifters in [12] and [14] and occupies less chip area than the passive phase shifters in [11] and [13].

VI. Conclusions

In this paper, we have proposed a new receiver architecture for hybrid beam-forming which splits the sampling task outside of the ADC and applies appropriate sampling offsets to provide analog beam-forming phase shifts. We have also presented low-overhead channel estimation based on judiciously selected antenna subset together with the low-complexity sampling offset computation algorithm. The proposed approach

TABLE II
COMPARISON OF DIFFERENT BEAM-FORMING RF PHASE GENERATION APPROACHES

	This Work	Yeh [9] JSSC'16	Yu [10] RFIC'09	Kodak [11] RFIC'16	Koh [12] JSSC'07	Shin [13] MWCL'16	Sumam [14] MTT'13
Technology	28nm CMOS	130nm SiGe	130nm CMOS	45nm CMOS	130nm CMOS	65nm CMOS	180nm CMOS
Phase Resolution	4-bit	4-bit	4-bit	5-bit	4-bit	4-bit	4-bit
Frequency (GHz)	28	28-32	24-27	26-28	15-26	27.5-28.35	15-35
Phase Error (°)	< 2.1	< 5.4	< 6	< 4	< 6.5	< 8.98	< 4.2
DC Power (mW)	0/3.5[I]	N/A[II]	N/A[II]	0	11.7	0	25.2
Chip area	721.3*μm^2	0.27*mm^2	0.067*mm^2	0.25*mm^2	0.14**mm^2	0.02*mm^2	0.19*mm^2

[I]Without/with the multi-phase clock generation module.
[II]Not available.

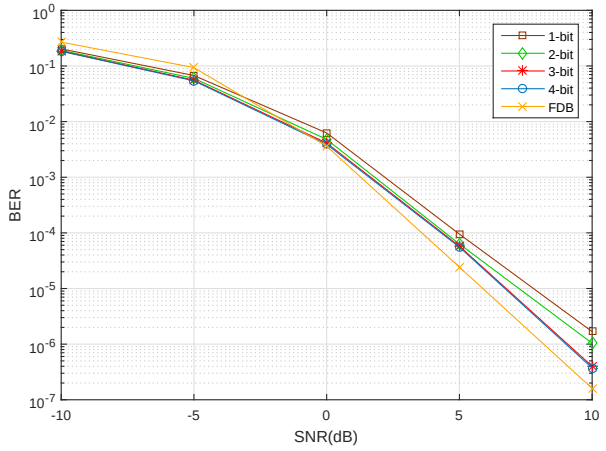

Fig. 7. BER performance of the proposed architecture with different phase resolutions and that of the FDB architecture which requires much higher power consumption and hardware complexity

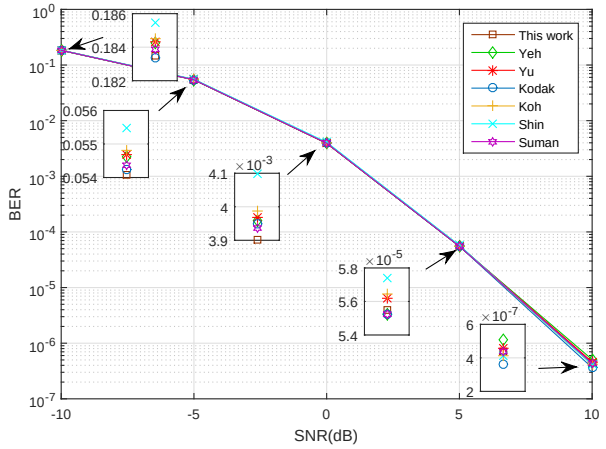

Fig. 8. BER performance of different phase generation methods

using RF under-sampling combined with the RF sampling offsets removes the need of mixers as well as chip area enlarging passive RF phase shifters or power consuming active RF phase shifters. Compared to the existing designs with RF phase shifters, the proposed design uses less power and chip area while obtaining the same BER performance. Future related works include applying a compressed sensing method for channel estimation to save the overhead and expanding the current design to multi-user cases.

REFERENCES

[1] W. Roh, J.-Y. Seol, J. Park, B. Lee, J. Lee, Y. Kim, J. Cho, K. Cheun, and F. Aryanfar, "Millimeter-wave beamforming as an enabling technology for 5G cellular communications: theoretical feasibility and prototype results," *IEEE Commun. Mag.*, vol. 52, no. 2, pp. 106–113, 2014.

[2] J. Zhang, X. Ge, Q. Li, M. Guizani, and Y. Zhang, "5G millimeter-wave antenna array: Design and challenges," *IEEE Wireless Communications*, 2016.

[3] X. Zhang, A. F. Molisch, and S.-Y. Kung, "Variable-phase-shift-based RF-baseband codesign for MIMO antenna selection," *IEEE Trans. Signal Process.*, vol. 53, no. 11, pp. 4091–4103, 2005.

[4] L. Wu, H. F. Leung, A. Li, and H. C. Luong, "A 4-Element 60-GHz CMOS phased-array receiver with beamforming calibration," *IEEE Trans. Circuits Syst. I, Reg. Papers*, 2016.

[5] D. M. Akos, M. Stockmaster, J. B. Tsui, and J. Caschera, "Direct bandpass sampling of multiple distinct RF signals," *IEEE Trans. Commun.*, vol. 47, no. 7, pp. 983–988, 1999.

[6] T. E. Bogale, L. B. Le, A. Haghighat, and L. Vandendorpe, "On the number of RF chains and phase shifters, and scheduling design with hybrid analog–digital beamforming," *IEEE Trans. Wireless Commun.*, vol. 15, no. 5, pp. 3311–3326, 2016.

[7] Z. Xu, S. Han, Z. Pan, and I. Chih-Lin, "Alternating beamforming methods for hybrid analog and digital MIMO transmission," in *International Conference Communications (ICC)*. IEEE, 2015, pp. 1595–1600.

[8] M. K. Samimi and T. S. Rappaport, "3-D statistical channel model for millimeter-wave outdoor mobile broadband communications," in *International Conference Communications (ICC)*. IEEE, 2015, pp. 2430–2436.

[9] Y.-S. Yeh, B. Walker, E. Balboni, and B. Floyd, "A 28-GHz Phased-Array Receiver Front End With Dual-Vector Distributed Beamforming," *IEEE J. Solid-State Circuits*, 2016.

[10] T. Yu and G. M. Rebeiz, "A 4-channel 24–27 GHz CMOS differential phased-array receiver," in *Radio Frequency Integrated Circuits Symposium (RFIC)*. IEEE, 2009, pp. 455–458.

[11] U. Kodak and G. M. Rebeiz, "A 42mw 26–28 GHz phased-array receive channel with 12 dB gain, 4 dB NF and 0 dBm IIP3 in 45nm CMOS SOI," in *Radio Frequency Integrated Circuits Symposium (RFIC)*. IEEE, 2016, pp. 348–351.

[12] K.-J. Koh and G. M. Rebeiz, "0.13-μm CMOS phase shifters for X-, Ku-, and K-band phased arrays," *IEEE J. Solid-State Circuits*, vol. 42, no. 11, pp. 2535–2546, 2007.

[13] G.-S. Shin, J.-S. Kim, H.-M. Oh, S. Choi, C. W. Byeon, J. H. Son, J. H. Lee, and C.-Y. Kim, "Low insertion loss, compact 4-bit phase shifter in 65 nm CMOS for 5G applications," *IEEE Microw. Compon. Lett*, vol. 26, no. 1, pp. 37–39, 2016.

[14] S. P. Sah, X. Yu, and D. Heo, "Design and analysis of a wideband 15–35-GHz quadrature phase shifter with inductive loading," *IEEE Trans. Microw. Theory Techn.*, vol. 61, no. 8, pp. 3024–3033, 2013.